

submitted to ApJL

HST/STIS Imaging of the Host Galaxy of GRB 980425/SN1998bw ¹

J. U. Fynbo

*Astronomical Observatory, University of Copenhagen, Juliane Maries Vej 30, DK-2100
Copenhagen Ø, Denmark*

`jfynbo@ifa.au.dk`

S. Holland

Institute of Physics and Astronomy, University of Aarhus, DK-8000 Århus C, Denmark

`holland@ifa.au.dk`

M. I. Andersen

*Division of Astronomy, University of Oulu, P. O. Box 3000, FIN-90014 University of Oulu,
Finland*

`manderse@sun3.oulu.fi`

B. Thomsen

Institute of Physics and Astronomy, University of Aarhus, DK-8000 Århus C, Denmark

`bt@ifa.au.dk`

J. Hjorth

*Astronomical Observatory, University of Copenhagen, Juliane Maries Vej 30, DK-2100
Copenhagen Ø, Denmark*

`jens@astro.ku.dk`

G. Björnsson

Science Institute, Dunhagi 3, University of Iceland, IS-107 Reykjavik, Iceland

`gulli@raunvis.hi.is`

A. O. Jaunsen

Institute of Theoretical Astrophysics, University of Oslo, Blindern, N-0315 Oslo, Norway

`a.o.jaunsen@astro.uio.no`

P. Natarajan

*Institute of Astronomy, Madingley Road, Cambridge CB3 0HA, England, and Department of
Astronomy, Yale University, New Haven, CT 06520–8181, U.S.A.*

`priya@ast.cam.ac.uk`

and

N. Tanvir

*Department of Physical Sciences, University of Hertfordshire, College Lane, Hatfield,
Hertfordshire AL10 9AB, England*

`nrt@ast.cam.ac.uk`

ABSTRACT

We present *HST*/STIS observations of ESO 184–G82, the host galaxy of the gamma-ray burst GRB 980425 associated with the peculiar Type Ic supernova SN1998bw. ESO 184–G82 is found to be an actively star forming SBc sub-luminous galaxy. We detect an object consistent with being a point source within the astrometric uncertainty of $0''.018$ of the position of the supernova. The object is located inside a star-forming region. The object is $\gtrsim 1$ magnitude brighter than expected for the supernova based on a simple radioactive decay model. This implies either a significant flattening of the light curve or a contribution from an underlying star cluster.

Subject headings: galaxies: individual (ESO 84–G182) — astrometry — supernovae: individual (SN1998bw) — gamma rays: bursts

1. Introduction

There is evidence that at least some gamma-ray bursts (GRBs) are related to supernovae (SNe). GRB 980425, GRB 970514 and GRB 980919 are consistent with being in temporal as well as spatial coincidence with SN1998bw, SN1997cy and SN1999E, respectively (Galama et al. 1998; Germany et al. 2000; Turatto et al. 2000; Thorsett & Hogg 1999). The associations between GRB 970514

¹Based on observations with the NASA/ESA *Hubble Space Telescope* (*HST*), obtained at the Space Telescope Science Institute, which is operated by the Association of Universities for Research in Astronomy, Inc. under NASA contract No. NAS5-26555 and on observations made with ESO Telescopes at the Paranal Observatory under programme ID 63.O-0065.

and SN1997cy, and between GRB 980919 and SN1999E, could be by chance. However, this is very unlikely for GRB 980425 since the temporal and spatial constraints are much tighter than for the two other possible GRB/SN associations (Galama et al. 1998). Furthermore, there is evidence for a contribution from SNe to the light-curves of GRB 970228 and GRB 980326 (Dar 1999; Reichart 1999; Bloom et al. 1999; Castro-Tirado & Gorosabel 1999; Galama et al. 2000). However, less than 0.2% of SNe release detectable gamma-ray emission (Kippen et al. 1998; Woosley et al. 1999), and SN1997cy, SN1998bw and SN1999E were extremely bright and peculiar SNe. This association between GRBs and peculiar SNe suggests that GRB 980425 (and possibly also GRB 970514 and GRB 980919) were members of a rare class of GRBs and may not be indicative of normal GRBs. However, the temporal and spatial properties of the gamma radiation from GRB 980425, except for the low total luminosity, were not unusual (Galama et al. 1998; Pian et al. 2000).

In this *Letter* we present Space Telescope Imaging Spectrograph (STIS) clear and long-pass images of the host galaxy of SN1998bw as part of a large survey aimed at studying the morphology of GRB host galaxies and the locations of the GRBs within the host galaxies. SN1998bw occurred in a spiral arm of the face-on SB galaxy ESO 184–G82 (Holmberg et al. 1977). The redshift of ESO 184–G82 is 0.0085 (Tinney et al. 1998). The aims of this *Letter* are to characterize the region in ESO 184–G82 where SN1998bw occurred, and to measure or constrain the brightness of SN1998bw at a late epoch more than two years after the event.

We use a Hubble parameter of $H_0 = 100h^{-1} \text{ km s}^{-1} \text{ Mpc}^{-1}$ and assume $\Omega_m = 0.3$ and $\Omega_\Lambda = 0.7$ throughout this *Letter*. For this cosmology a redshift of $z = 0.0085$ corresponds to a luminosity distance of $25.65h^{-1} \text{ Mpc}$ and a scale of $122h^{-1} \text{ proper parsecs per arcsecond}$.

2. Observations and Data Reductions

The *Hubble Space Telescope* (*HST*) was used to obtain STIS/CCD images of ESO 184–G82 between 21:47 UT and 23:42 UT on 11 June 2000 (Holland et al. 2000b). A log of the *HST* observations is given in Table 1. The total exposure times were 1240 seconds in the 50CCD (clear, hereafter referred to as CL) aperture and 1185 seconds in the F28X50LP (long pass, hereafter referred to as LP) aperture². The CCD gain was set to 1 e[−]/ADU and the read-out noise was 4.46 ADU/pixel. The data was processed through the standard STIS pipeline and combined using the DITHER (v1.2) software (Fruchter & Hook 2000) as implemented in IRAF³ (v2.11.1)/STSDAS (v2.0.2). We used “pixfrac” = 0.6 and a final output scale of 0″.0254/pixel. These observations were taken as part of the Cycle 9 program GO-8640: Survey of the Host Galaxies of Gamma-Ray Bursts.

²The 50CCD aperture has a central wavelength of 5850 Å and a width of 4410 Å. The F28X50LP aperture has a central wavelength of 7230 Å and a width of 2720 Å (STIS Handbook v4.1)

³Image Reduction and Analysis Facility (IRAF), a software system distributed by the National Optical Observatories (NOAO).

The URL for the survey is http://www.ifa.au.dk/~hst/grb_hosts/index.html (Holland et al. 2000a).

3. Results

The drizzled CL image is shown as Fig. 1. ESO 184–G82 is a barred spiral galaxy of Hubble type SBc (Rautiainen 2000). The magnitude of the galaxy is $B = 15.19 \pm 0.05$, $R = 14.28 \pm 0.05$ (Lauberts & Valentijn 1989), which corresponds to $L_B = 0.02L_B^*$ using $M_B^* = -21.2 + 5 \log_{10}(h)$ (Marinoni et al. 1999).

The galaxy is clearly in a stage of active star formation. Fig. 1 shows that the optical appearance of the galaxy is dominated by a large number of high surface brightness star forming regions especially in the southern spiral arm where the SN occurred. When comparing the CL and LP images a large number of red giants can be seen within or near the star forming regions (two examples are seen in Fig. 2).

As also noted by Holmberg et al. (1977) ESO 184–G82 is member of a group of galaxies consisting of the three galaxies ESO 184–G80, ESO 184–G81 and ESO 184–G82. Furthermore, there is an previously unclassified Sb galaxy 1.'1 south of ESO 184–G82 and a fainter bulge-dominated galaxy 1.'7 south of ESO 184–G82. Hence, the star formation activity could be enhanced by interaction (see § 4).

3.1. Astrometry

The most precise determination of the absolute position of SN1998bw on the sky is based on the radio observations made with the Australian Telescope Compact Array April 28 1998 (Wieringa et al. 1998). This position is RA = 19:35:03.31, Dec. = $-52:50:44.7$ (J2000.0) with an error of 0".1. However, SN1998bw was very faint at the time of the STIS observations, and there are no other sources in the STIS Field of View (FOV) for which positions have been determined with equally high precision. In order to determine relative astrometry between SN1998bw and other objects in the STIS FOV we therefore retrieved images obtained with the ESO-VLT Antu telescope with the FORS1 instrument from the ESO archive. These images were taken at an epoch (1999 April 18) when the SN was still clearly visible. The journal of archive data is given in Table 2 (Leibundgut et al. 2000; Sollerman et al. 2000).

The precise location of the SN in the STIS CL image was derived from the ground based VLT images in the following way. The STIS images revealed several bright blue objects within 0".5 of the position of the SN. These objects were covered under the point-spread function (PSF) in the VLT images, which had a seeing of about 0".9. This affected the centroid determination of the SN somewhat, giving rise to a colour dependent position error of ≈ 1.5 drizzled STIS pixels ($\approx 0".038$).

By smoothing, scaling, and transforming the STIS CL and LP images, the contribution from the host galaxy, including the clusters in the proximity of the SN, could be subtracted completely from the VLT *V* and *I* images. Astrometry, based on these two subtracted images, gave accurate and internally consistent positions, based on six and eleven reference stars. The fits are six-parameter affine fits, with weights calculated from a noise model. The errors are the standard deviations of the residuals in the fit, properly normalized by weights and degrees of freedom. The final error of the weighted position was estimated to be about 0.7 drizzled pixels in the CL image, or about $0''.018$. In the drizzled LP the error is slightly smaller.

In order to check this position DAOPHOT II (Stetson 1987, 1999) with extensions (DAOMATCH and DAOMASTER) was applied to the drizzled STIS LP image and the ground based VLT *R* image, respectively. Subsequently the two auxiliary programs DAOMATCH and DAOMASTER were used to derive a four-parameter transformation (offset, scale and orientation) from the positions of five isolated stars judged to be free of superposed nebulosities. The transformed position of the SN is within 0.5 pixels of the value derived from our more formal astrometric procedure.

3.2. The Environment of the SN

As also noted by Leibundgut et al. (2000) and Sollerman et al. (2000) the SN is superposed on an H II region. The diameter of this region is approximately between $2''$ and $3''$, corresponding to a physical diameter of between $250h^{-1}$ and $350h^{-1}$ pc at $z = 0.0085$. Fig. 2a shows a region with a size of $1''.0 \times 1''.0$ centered on the position of the SN as determined in Sect. 3.1. At the exact position of the SN is the object marked by an arrow in Fig. 2a. The object is also seen in the LP image shown in Fig. 2c. In the following we will refer to this object as the SN. Also seen are six objects (in the following referred to as s1–s6) consistent with being point sources. In the CL image there appears to be an arc-like structure extending from the SN towards s6.

3.3. Photometry and PSF-Subtraction

We estimated the total AB magnitude of the SN, the other point sources (s1–s6) visible in Fig. 2 and the arc-like structure, on both the CL and LP images in the following way. For the photometry of the point sources we use DAOPHOT II. We determined the PSF in the same way as described in § 4 of Holland & Hjorth (1999). We used ALLSTAR (Stetson & Harris 1988) with a fitting radius of $0''.071$ and a sky annulus of $0''.076$ – $0''.178$ to fit a PSF to the object and determined aperture corrections by measuring the magnitudes of several stars in apertures with radii of $1''.108$ (CL) and $0''.963$ (LP). Tables 14.3 and 14.5 of the STIS Instrument Handbook show that these radii correspond to $\approx 100\%$ of the encircled energy for a point source. We used the STIS zero points given in (Gardner et al. 2000) to convert the count rates to CL and LP magnitudes. We transformed the CL and LP magnitudes to Johnson *V* and Kron–Cousins *I* magnitudes using the

calibrations of (Rejkuba et al. 2000). They used 33 stars with $-0.8 < V - I < 2.0$ and found that the RMS residuals of their calibrations were $\sigma_V = 0.24$ and $\sigma_I = 0.17$.

As seen in Fig. 2b and Fig. 2d all seven objects, including the probably SN remnant in the error ellipse, are well subtracted by the PSF. The results of our PSF-photometry are given in Table 3. The uncertainties in the V and I magnitudes are dominated by the uncertainties in the transformations from CL and LP. The ΔX and ΔY values are the coordinates on the drizzled STIS CL image of each object relative to the SN remnant. The colours of s2 and s4 are consistent with red giant stars whereas the other four point sources have blue colours consistent with massive main-sequence stars.

We measured the surface brightness of the arc-like structure in the following way. We subtracted the point sources in Table 3 and smoothed the resulting images with a Gaussian with a full-width at half-maximum of three pixels. We then fit-by-eye a line through the arc and measured the mean countrate along this line. The sky was estimated from empty regions of the CL and LP images. The results of this procedure are $\mu_V = 21.9 \pm 0.3$ and $\mu_I = 20.3 \pm 0.3$, yielding $V - I = 1.6 \pm 0.4$. This structure might be the source of the $H\alpha$ emission seen in late spectra of SN1998bw (Sollerman et al. 2000)

4. Discussion

4.1. The Afterglow of GRB980425/SN1998bw

GRB 980425/SN1998bw occurred in the southern spiral arm of the sub-luminous ($L_B = 0.02L_B^*$), barred SBc galaxy ESO 184-G82. This galaxy is in a stage of strong star formation. In this way ESO 184-G82 resembles the LMC, which is also sub-luminous, barred and dominated by regions with strong star formation. We note that ESO 184-G82 is $\approx 0.3h^{-2}$ as luminous as the LMC. For $H_0 = 50-80 \text{ km s}^{-1} \text{ Mpc}^{-1}$ (de Bernardis et al. 2000) ESO 184-G82 has a luminosity of $\approx 0.5-1.2L_{\text{LMC}}$.

There are two possible explanations for why ESO 184-G82 is undergoing strong star formation. These explanations may be related. Firstly, ESO 184-G82 has a bar. Whereas the presence of a bar in spiral galaxies does not, in general, correlate with the global star formation rate (Kennicutt 1998) the bar strength has been found to correlate strongly with the global star formation rate of the galaxy (Aguerre 1999). Secondly, although we only have a measured redshift for ESO 184-G82 (Tinney et al. 1998), the galaxy is probably member of a group of at least five galaxies simply based on the low likelihood of a chance projection. The nearest neighbour is an Sb galaxy at a projected separation of only $8.3h^{-1} \text{ kpc}$. Moreover, ESO 184-G82 shows indications of being morphologically disturbed. Interaction induced star formation is therefore a likely explanation.

The SN occurred in a star-forming region with several bright, young stars within a projected distance of $\sim 100 \text{ pc}$. In this respect, it is similar to most core-collapse SNe that typically are

located within young stellar associations in spiral arms (Barth et al. 1996; Van Dyk et al. 1999).

The magnitude of the emission at the position of the SN 778 days after the discovery of the GRB is $\gtrsim 1$ magnitude brighter than one would expect from a simple radioactive decay model (Sollerman et al. 2000). The emission in both the CL and LP image is well-fitted by a PSF at a position that is consistent with the precise position of the SN determined in § 3.1. The residuals remaining after subtracting the scaled PSF are consistent with noise. This suggests that the majority of the observed emission could in fact be from the SN. We tested our ability to resolve a star cluster in ESO 184–G82 by adding artificial clusters with Michie–King (Michie 1963; King 1966) profiles and the same flux as the SN remnant to the CL image as described in (Holland et al. 1999). We found that star clusters with core radii of $r_c \gtrsim 0''.013$ ($= 1.6h^{-1}$ pc) appeared as extended objects and are not well fit by the PSF. This suggests that, if the SN did occur in a star cluster, the underlying star cluster is either physically very small and thus can not be distinguished from a point source, or that the underlying star cluster is very faint. If the emission is really dominated by the fading SN, as can only be confirmed by follow-up observations with the *HST*, this would imply a significant flattening of the light curve, possibly explained by interaction with circumstellar material or accretion on a black hole (Leibundgut et al. 2000; Parat et al. 2000; Sollerman et al. 2000), or the effect of the positron decay (Nakamura et al. 2000).

4.2. Implications for GRB-Research

These data provide a very solid confirmation of the hypothesis that at least some GRBs are strongly related to star formation (Paczynski 1998). However, some GRBs, such as GRB 970508, show evidence that there was no SN like SN1998bw associated with them. Therefore, either GRBs are associated with non-standard-candle SNe, or only some GRBs are associated with SNe and the others have a different progenitor. Graziani et al. (1999) have used Bayesian methods to estimate that no more than $\approx 5\%$ of the GRBs that have been detected by BATSE were produced by known SNe Ib–Ic. However, (Galama et al. 1998) conservatively estimate the probability that the coincidence between GRB 980425 and SN1998bw is chance to be $\approx 10^{-4}$. This suggests that GRB980425/SN1998bw was a member of an unusual class of GRBs/SNe.

GRB 980425 had a isotropic-equivalent energy of 10^{48} erg (Pian et al. 2000), making it $\approx 10^4$ less energetic than the other GRBs for which distances (and thus isotropic-equivalent energies) have been determined. If GRB 980425 had occurred at $z = 1$ (the median redshift of the GRBs with measured redshifts) it would not have been detected. As of 30 June 2000 redshifts and total isotropic energies have been determined for only ten GRBs, with nine having energies between 2×10^{51} erg and 3×10^{54} erg, and one having an energy of 10^{48} erg. If we assume that this ratio holds for the entire BATSE 4B Catalogue (Paciesas et al. 1999) then the observed number of high-energy ($E \geq 10^{51}$ erg) GRBs with known redshifts (nine) implies that a high-energy GRB will occur at $z \lesssim 0.01$ only once every $\approx 20\,000$ years. Therefore, it is not surprising that we have not observed any high-energy GRBs with $z \lesssim 0.01$. GRBs with isotropic-equivalent energies of $\approx 10^{48}$

may be common at $z \gtrsim 1$, but are undetectable with current instruments.

We thank J. Sollerman and our anonymous referee for several useful comments that improved our manuscript on several important points. We also thank P. Rautiainen for determining the Hubble type of ESO 184–G82. This work was supported by the Danish Natural Science Research Council (SNF).

REFERENCES

- Aguerri, J. A. L., 1999, A&A, 351, 43
- Barth, A.J., Van Dyk S.D., Filippenko, A.V., Leibundgut, B., Richmond, M.W., 1996, AJ, 111, 2047
- Bloom, J. S., et al., 1999, Nature, 401, 453
- Castro-Tirado, A. J., & Gorosabel, J., 1999, A&AS, 138, 449
- Dar A., 1999, GCN 346
- de Bernardis, P., et al., 2000, Nature, 404, 955
- Fruchter, A. S., Hook, R. N., 2000, PASP, in press, astro-ph/9808087
- Galama, T. S., et al., 1998, Nature, 395, 670
- Galama, T. S., et al., 2000, ApJ, 536, 185
- Gardner, J. P., et al., 2000, AJ, 119, 486
- Germany, L. M., Reiss, D. J., Sadler, E. M., Schmidt, B. P., & Stubbs, C. W., 2000, ApJ, 533, 320
- Graziani, C., Lamb, D. Q., and Marion, G. H., 1999, A&AS, 138, 469
- Holland, S., Côté, P., & Hesser, J. E., 1999, A&A, 348, 418
- Holland, S., & Hjorth, J., 1999, A&A 344, L67
- Holland, S., et al., 2000a, GCNC 698
- Holland, S., et al., 2000b, GCNC 704
- Holmberg, E. B., Lauberts, A., Schuster, H. E., & West, R. M., 1977, A&AS 27, 295
- Kennicutt, R. C., 1998, ARA&A 36, 189
- King, I. R., 1966, AJ, 71, 64

- Kippen, R. M., et al., 1998, ApJ 506, L27
- Lauberts, A., & Valentijn, E. A., 1989, The Surface Photometry Catalogue of the ESO-Uppsala Galaxies, ESO: Garching
- Leibundgut, B., et al., 2000, The ESO Messenger, 95, 36
- Marinoni, C., Monaco, P., Giuricin, G., & Costantini, B., 1999, ApJ 521, 50
- Michie, R. W., 1963, MNRAS, 125, 127
- Nakamura, T., Mazzali, P. A., Nomoto, K., & Iwamoto, K., 2000, ApJL, submitted, astro-ph/0007010
- Paczynski, B., 1998, ApJ, 494, L45
- Patat, F., et al., 2000, IAUC 7215
- Paciesas, W. S., et al., 1999, ApJS, 122, 465
- Pian, E., et al., 2000, ApJ, 536, 778
- Rautiainen P., 2000, private communication
- Reichart, D. E., 1999, ApJ, 521, L111
- Rejkuba M., Minniti D., Gregg M. D., Zijlstra A. A., Alonso M. V., Goudfrooij P., 2000, AJ, in press, astro-ph/0004231
- Sollerman, J., et al., 2000, ApJL, in press, astro-ph/0006406
- Stetson, P. B. 1987, PASP, 99, 191
- Stetson, P. B. 1999, private communication
- Stetson P. B., Harris W. E., 1988, AJ, 96, 909
- Thorsett, S. E., & Hogg, D. W., 1999, GCNC 197
- Tinney, C., Stathakis, R., Cannon, R., & Galama, T.J., 1998, IAUC 6896
- Turatto, M., et al., 2000, ApJ, 534, L57
- Van Dyk, S.D., Peng, C.Y., Barth, A.J., Filippenko, A.V., 1999, AJ, 118, 2331
- Woosley, S. E., Eastman, R. G., & Schmidt, B. P., 1999, ApJ 516, 788
- Wieringa, M., Frail, D. A., Kulkarni, S. R., Higdon, J. L., & Wark, R., 1998, GCNC 63

Table 1. The journal of *HST*/STIS observations

Field	Date (UT)	Aperture	Exposure Time (s)
GRB 980425	2000 Jun 11	50CCD (CL)	1×60 4×295
GRB 980425	2000 Jun 11	F28X50LP (LP)	3×296 1×297

Table 2. Log of FORS1 observations from the VLT-archive

Field	Date (UT)	Filter	Seeing (arcsec)	Exposure Time (s)
GRB 980425	1999 Apr 18	<i>V</i>	0.93	30
GRB 980425	1999 Apr 18	<i>R</i>	0.89	30
GRB 980425	1999 Apr 18	<i>I</i>	0.89	45

Table 3. Results of PSF-photometry of the objects seen in Fig. 2

Object	ΔX	ΔY	CL_{AB}	LP_{AB}	<i>V</i>	<i>I</i>
SN	0.0	0.0	25.42 ± 0.06	25.51 ± 0.08	25.41 ± 0.25	24.39 ± 0.19
s1	−14.6	17.5	25.02 ± 0.04	25.56 ± 0.08	24.89 ± 0.24	24.67 ± 0.19
s2	−11.2	15.4	25.88 ± 0.07	25.08 ± 0.04	26.10 ± 0.25	23.50 ± 0.17
s3	−7.4	10.4	25.31 ± 0.04	25.70 ± 0.10	25.22 ± 0.24	24.73 ± 0.20
s4	10.6	3.0	25.90 ± 0.06	25.28 ± 0.06	26.07 ± 0.25	23.79 ± 0.18
s5	−16.5	−13.8	24.93 ± 0.03	25.06 ± 0.05	24.91 ± 0.24	23.96 ± 0.18
s6	−0.9	−14.4	25.27 ± 0.04	25.10 ± 0.05	25.32 ± 0.24	23.84 ± 0.18

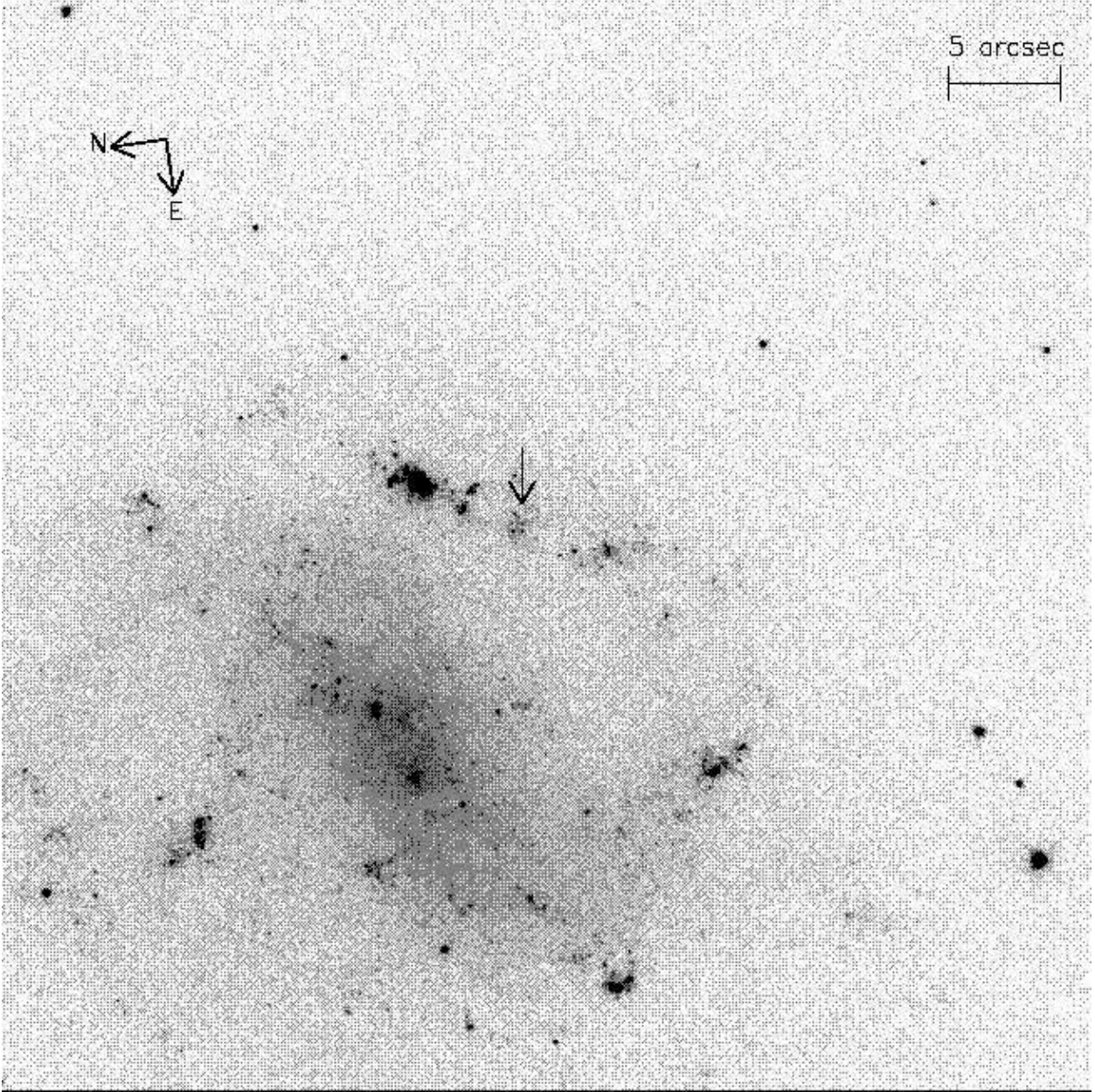


Fig. 1.— The drizzled CL image. The total size of the image is $49'' \times 49''$. The orientation of the field is shown in the upper left corner of the image. The position angle is $188^\circ.25$ East of North. The arrow marks the position of the SN (§ 3.1).

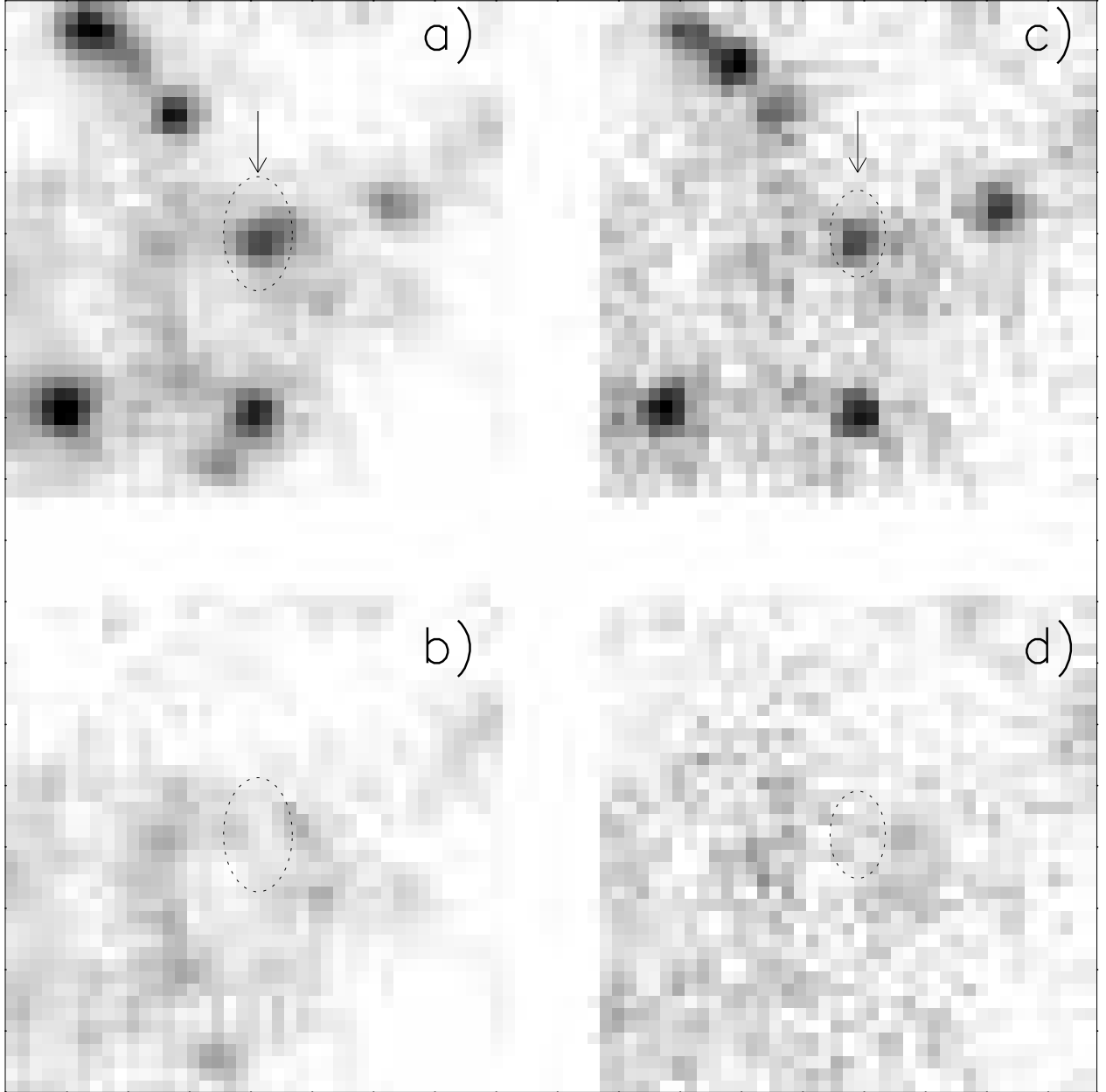


Fig. 2.— The orientation of each panel is the same as if Fig. 1. *a)* A region of 40×40 drizzled pixels ($1''.0 \times 1''.0$) centered on the position of the SN from the CL image. The orientation of the field is the same as in Fig. 1. The 5σ error-ellipse for the astrometry is shown as a dotted ellipse. The region marked by an arrow is consistent with the position of the SN to within the astrometric error. Also seen in the field are the six objects (s1–s6) consistent with being point sources (see Table 3). Three of these (s2, s4, and s6) have colours consistent with being red giant stars. The other three point sources have blue colours that are consistent with massive main-sequence stars. There is also an arc-like structure extending from the SN towards s6. *b)* The same region as in *a)* after subtraction of the seven PSFs as described in Sect. 3.3. *c)* and *d)* Same as *a)* and *b)*, but for the LP image.